

# Disentangling Scaling Properties in Anisotropic Fracture

Eran Bouchbinder, Itamar Procaccia and Shani Sela

*Dept. of Chemical Physics, The Weizmann Institute of Science, Rehovot 76100, Israel*

Structure functions of rough fracture surfaces in isotropic materials exhibit complicated scaling properties due to the broken isotropy in the fracture plane generated by a preferred propagation direction. Decomposing the structure functions into the even order irreducible representations of the  $SO(2)$  symmetry group (indexed by  $m = 0, 2, 4, \dots$ ) results in a lucid and quickly convergent description. The scaling exponent of the isotropic sector ( $m = 0$ ) dominates at small length scales. One can reconstruct the anisotropic structure functions using only the isotropic and the first non vanishing anisotropic sector ( $m = 2$ ) (or at most the next one ( $m = 4$ )). The scaling exponent of the isotropic sector should be observed in a proposed, yet unperformed, experiment.

**Introduction:** Imagine a fracture experiment in which an initial circular cavity is made to propagate by a tensile load such that the crack edge remains circular on the average, without any preferred propagation direction in the plane normal to the load, see Fig. 1. From the point of view of the scaling properties of the rough fracture surface that is left behind the advancing crack, such an experiment is the analogue of homogenous and isotropic turbulence in nonlinear fluid mechanics. Normal experiments in both fracture and turbulence involve symmetry breaking; the boundary conditions introduce anisotropy, making the discussion of scaling properties non-trivial. In turbulence it was shown how to disentangle the anisotropic contributions from the isotropic one by projecting the measured correlation and structure functions on the irreducible representations of the  $SO(3)$  symmetry group [1]. The scaling phenomena seen in the isotropic sector of anisotropic experiments are identical to those expected in the hypothetical experiment of homogenous and isotropic turbulence. The aim of this Letter is to introduce a similar concept to the field of fracture: we will show that decomposing the height-height structure functions of fracture surfaces into the irreducible representations of the  $SO(2)$  symmetry group results in a simplification and rationalization of the scaling properties that is not totally dissimilar to the one obtained in turbulence. The scaling properties of the isotropic sector should be observable in principle in an experiment like the one shown in Fig. 1, which contrary to turbulence may be performed in reality.

The pioneering experimental work described in Ref. [2] drew attention to the fact that fracture surfaces are graphs in 2+1 dimensions when the broken sample is three dimensional. This initial insight was followed up by a considerable number of works [3] that focused on the scaling properties of such graphs under affine transformations. In 2+1 dimensions one denotes the graph as  $h(\mathbf{r})$  and considers the structure function  $S_2(\ell)$ ,

$$S_2(\ell) \equiv \langle (h(\mathbf{r} + \ell) - h(\mathbf{r}))^2 \rangle, \quad (1)$$

where angular brackets denote an average over all  $\mathbf{r}$ . Initially no attention was paid to the fact that the

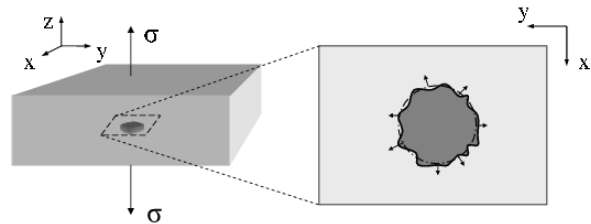


FIG. 1: Sketch of a hypothetical fracture experiments arranged to allow a crack to develop in an isotropic fashion, i.e. with all angles  $\theta$  being statistically equivalent. On the left, the full three dimensional experiment is shown, where the tensile axis is along  $z$  and a circular cavity is in the  $xy$  plane. On the right, a magnified version of the circular cavity in the  $xy$  plane is shown.

isotropy in the fracture plane is broken due to initial conditions that lead to a preferred propagation direction, and the statement of [2] was that the structure function is a homogeneous function of its arguments,  $S_2(\lambda\ell) \sim \lambda^{\zeta^{(2)}} S_2(\ell)$ . In fact such a statement is tenable only if the fracture process *and* the material are isotropic. Usually the crack propagates predominantly in one direction (say  $\hat{\mathbf{x}}$ ) and the vector  $\ell$  defines an angle  $\theta$  with respect to  $\hat{\mathbf{x}}$ ,  $\theta = \cos^{-1}(\hat{\mathbf{x}} \cdot \hat{\ell})$ . There is no reason why the scaling exponent  $\zeta^{(2)}$ , if it exists at all, should not depend on the angle  $\theta$ . Indeed, in the later work that followed [2] this problem was recognized and scaling exponents were sought for one dimensional cuts through  $S_2(\ell)$ , typically parallel and orthogonal to the direction of the crack propagation. Besides the obvious meaning of ‘parallel’ and ‘orthogonal’ to  $\hat{\mathbf{x}}$ , no reason was ever given why these particular directions are expected to provide clean scaling properties. We will argue below that in general such one dimensional cuts exhibit a mixture of scaling exponents with amplitudes that depend on the angle  $\theta$ , where  $\theta = 0$  and  $\theta = \pi/2$  are not special.

**Approach:** Given an experimental surface  $h(\mathbf{r})$  we

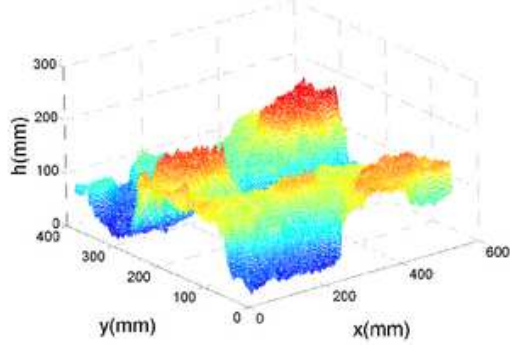


FIG. 2: The raw fracture surface of the aluminum alloy obtained in Ref. [4].

first compute the second order structure function Eq. (1). The vector  $\ell$  is associated with a norm  $\ell$  and an angle  $\theta$ . By construction, the second order structure function is symmetric under  $\theta \rightarrow \theta + \pi$ . Accordingly, decomposing the structure functions into the irreducible representations of the  $SO(2)$  symmetry group results in summations over even indices only:

$$S_2(\ell, \theta) = \sum_{m=-\infty}^{\infty} a_{2m}(\ell) e^{i2m\theta}. \quad (2)$$

Such a decomposition is deemed useful when each of the scalar functions  $a_{2m}(\ell)$  is itself a homogeneous function of its argument, characterized by an  $m$  dependent exponent:

$$|a_{2m}(\lambda\ell)| \sim \lambda^{\zeta_{2m}^{(2)}} |a_{2m}(\ell)|, \quad (3)$$

where  $|\cdot|$  stands for the norm of a complex number. For an isotropic fracture in an isotropic medium we expect  $a_{2m}(\ell) = 0$  for all  $m \neq 0$ . In usual mode I experiments in which the crack propagates along the  $\hat{x}$  direction and the tensile load is in the normal direction, there should be the same physics along lines with angles  $\theta$  and  $-\theta$ . This invariance under  $\theta \rightarrow -\theta$  implies that the arguments of all  $a_{2m}(\ell) \neq 0$  should be 0 or  $\pi$ . In reality this invariance might not hold on large length scales due to the paucity of data or different experimental configurations.

**Example: aluminum alloy** - Our first example was obtained [4] from a compact tension specimen made of 7475 aluminum alloy first precracked in fatigue and then broken under tension in mode I. The raw fracture surface and the second order structure function computed from it are shown in Figs. 2 and 3 respectively. One sees the anisotropy of  $S_2(\ell)$  with the naked eye. To quantitatively characterize this anisotropy, the structure function was decomposed as in Eq. (2). The log-log plots of  $a_0(\ell)$ ,  $2|a_2(\ell)|$  and  $2|a_4(\ell)|$  are exhibited in Fig. 4. By performing linear fit of the relevant range in the log-log plots we find the following exponents

$$\zeta_0^{(2)} = 1.32 \pm 0.07, \zeta_2^{(2)} = 1.45 \pm 0.08, \zeta_4^{(2)} = 2.1 \pm 0.1. \quad (4)$$

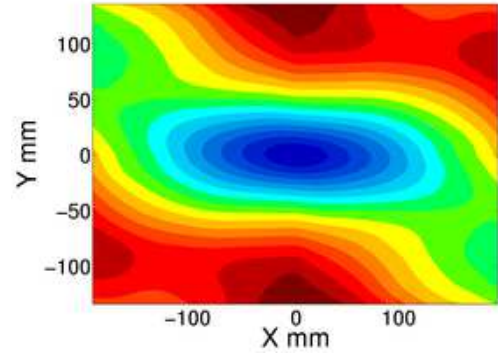


FIG. 3: Contour plot of the second order structure function of the surface shown in Fig. 2.

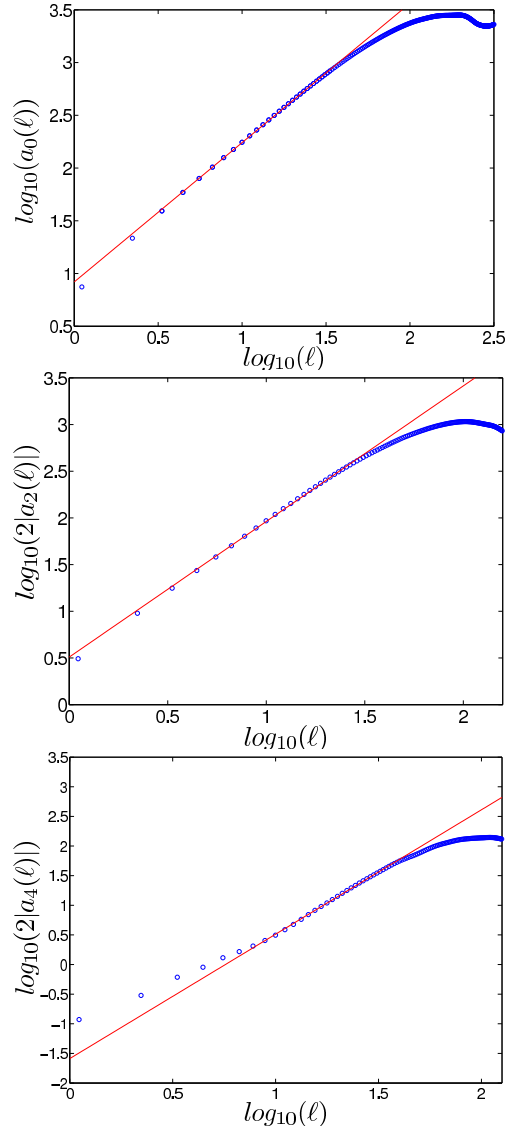


FIG. 4: Log-log plots of the amplitudes  $a_0(\ell)$ ,  $2|a_2(\ell)|$  and  $2|a_4(\ell)|$  vs.  $\ell$  for the aluminum alloy.

The implication is that at smaller length-scales the smaller exponent  $\zeta_0^{(2)}$  should be dominant and vice versa. Indeed, examining again the contour plot in Fig. 3 one observes that at small scales the contours tend to ellipses of smaller eccentricity, whereas at larger scale the contours are ellipses with increasing eccentricity.

The crucial test of this approach is whether one can reconstruct the structure function  $S_2(\ell, \theta)$  using the functional form of the irreducible representation and a minimal number of parameters. Indeed, at smaller values of  $\ell$  the first two irreducible representations suffice. Writing

$$S_2(\ell, \theta) \approx 8.30 \ell^{1.32} + 3.22 \ell^{1.45} \cos(2\theta + \pi), \quad (5)$$

we compare in Fig. 5 the experimental data to Eq. (5) for  $\ell = 5, 15$  and  $25\text{mm}$ . The excellent fit is obvious. In fact, with four parameters (two amplitudes and two exponents) we can represent the structure function to within 1% in  $L^2$  norm as long as  $\ell \leq 30\text{mm}$ . For larger values of  $\ell$  the agreement decreases, and we need to employ the next irreducible representation. Adding  $0.026 \ell^{2.1} \cos(4\theta + \pi)$ , we find the fit shown in Fig. 6 for  $\ell = 35\text{mm}$ . Beyond these values the power-laws fits lose their credibility for this experimental data set.

**Example: artificial rock-** The second example was obtained from the fracture of artificial rocks produced from carbonatic aggregates cemented by epoxy [5]. The samples are plates of size  $400 \times 400 \times 9\text{ mm}$ , and the fracture surface was measured using a scanning laser profilometer. The analysis of the experimental data follows verbatim the first example. The plots of  $a_0(\ell)$  and  $2|a_2(\ell)|$  are shown in Fig. 7. Fitting the plots we find

$$\zeta_0^{(2)} = 0.86 \pm 0.05, \zeta_2^{(2)} = 1.93 \pm 0.05, \zeta_4^{(2)} = 1.93 \pm 0.1. \quad (6)$$

Two comments are in order. First, one should notice the non-universality of the scaling exponents as compared with the previous example (4). Second, the present surface does *not* satisfy a  $\theta \rightarrow -\theta$  symmetry. This may be either because the crack did not propagate strictly in the  $x$ -direction, or that the experimental data treatment destroyed this symmetry. Due to the lack of symmetry the amplitudes of the coefficient  $a_m$  can take any phase, not constrained to 0 or  $\pi$  as required by the  $\theta \rightarrow -\theta$  symmetry. The lack of symmetry is clearly obvious in the reconstruction of the structure function from the irreducible representations. In Fig. 8 we compare the experimental values of  $S_2(\ell, \theta)$ , for  $\ell = 2\text{ mm}$ , to the expansion

$$S_2(\ell, \theta) \approx 0.025 \ell^{0.86} + 0.0016 \ell^{1.93} \cos(2\theta + 2.09) + 5.4 \times 10^{-4} \ell^{1.93} \cos(4\theta - 0.17), \quad (7)$$

The fit is satisfactory and the asymmetry in  $\theta$  is obvious.

Taking the present two examples as representative, it appears that the SO(2) decomposition extracts pure scaling behavior in each sector, but that the scaling exponents are not universal, at least in the two materials

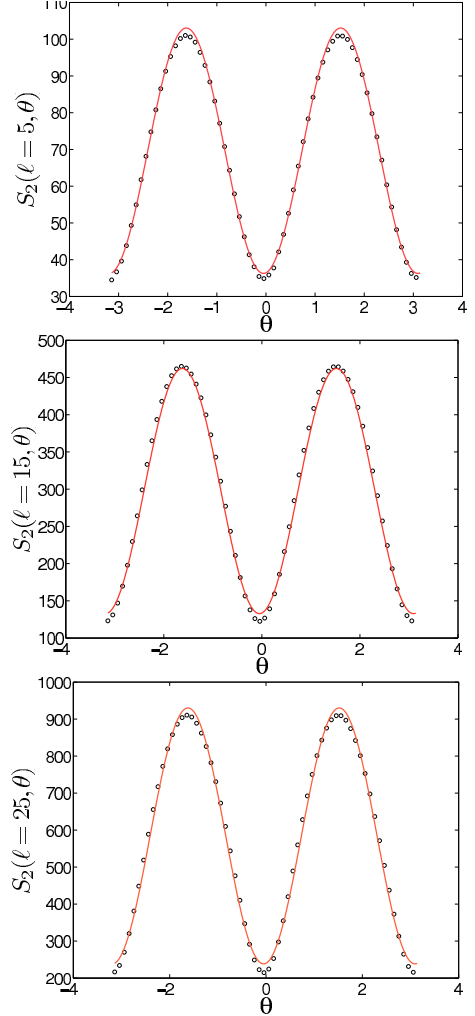


FIG. 5: The experimental  $S_2(\ell, \theta)$  for the aluminum alloy (circles) and the representation Eq. (5) (line), for  $\ell = 5, 15$  and  $25\text{mm}$ .

discussed here. Considering cuts in  $S_2(\ell, \theta)$  along the  $\theta = 0$  and  $\theta = \pi$  directions, the present approach predicts a mixture of scaling exponents rather than pure power laws. If we accept this prediction, it is worrisome that the averages of the two leading scaling exponents in the present two examples, i.e.  $(1.32+1.45)/2=1.38$  and  $(0.86+1.93)/2=1.39$  are very close. With the relatively short scaling range this may lead to an appearance of universality which the large differences in material structures and properties may not warrant.

Finally, one should point out that the SO(2) decomposition is not expected to yield satisfactory results when the material itself is strongly anisotropic. As an example we considered fracture surfaces in wood. This is clearly an anisotropic medium due to the fiber structure, and indeed we found that along and across the fiber structure the scaling behavior appears credible, whereas the SO(2) decomposition failed altogether to reveal clean scaling properties in any sector.

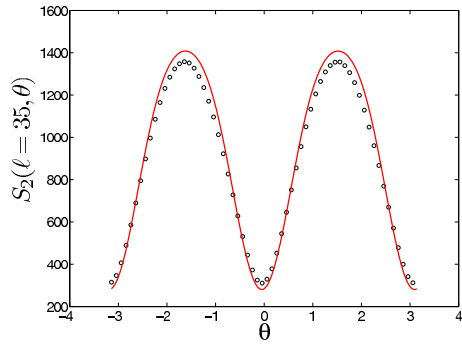


FIG. 6: The experimental  $S_2(\ell, \theta)$  for the aluminum alloy (circles) and the  $SO(2)$  expansion up to the third even order irreducible representation (line), for  $\ell = 35\text{mm}$ .

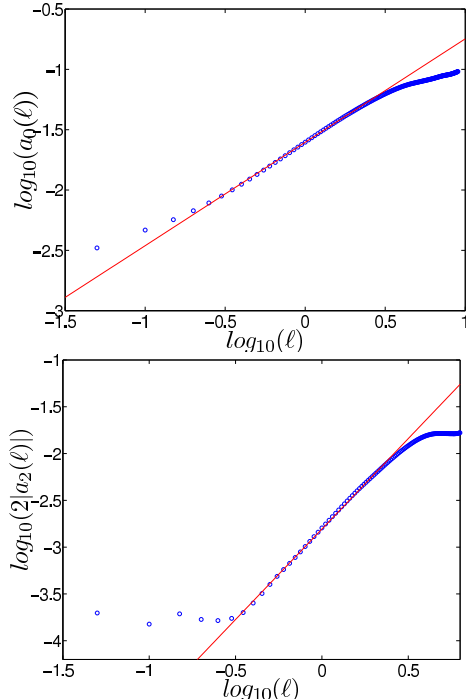


FIG. 7: Log-log plots of the amplitudes  $a_0(\ell)$  and  $2|a_2(\ell)|$  for the artificial rock.

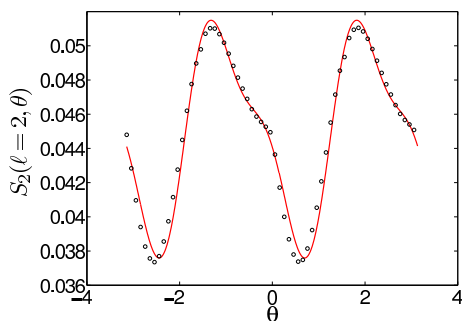


FIG. 8: Comparison of the experimental  $S_2(\ell, \theta)$  (circles) and the  $SO(2)$  expansion up to the third even irreducible representation (line) for the artificial rock with  $\ell = 2\text{mm}$ .

**Summary:** we propose that materials which can be fractured in an isotropic fashion, i.e materials having an isotropic structure, often have anisotropic fracture surfaces only because of the breaking of isotropy by the initial conditions. In such cases it appears useful to analyze the anisotropic contributions as “corrections to scaling” beyond the isotropic sector, which is always there, with a leading scaling exponent. The analysis reveals non-universality in the scaling exponents, a finding that calls for further future study and assessment, including the interesting question of the possible existence of universality classes. On the practical side, we have demonstrated that the full information concerning the two dimensional structure function can be efficiently parameterized by a few amplitudes and scaling exponents. The reader should note that this Letter dealt only with second order structure functions. In analogy to turbulence it may be possible to decompose any higher order structure function into  $SO(2)$  irreducible representations [7]. This may reveal additional interesting scaling properties such as the phenomenon of multiscaling [6]. Finally, we would like to emphasize the great interest in the proposed isotropic fracture experiment and the measurement of the roughness exponent in such an experiment. If indeed this scaling exponent were identical to the exponent of the isotropic sector in a standard experiment, this would significantly strengthen the theoretical interest in the approach proposed in this Letter.

**Acknowledgments:** We are grateful to D. Bonamy, E. Bouchaud, J. Fineberg and A. Sagiv for sharing with us their valuable experimental fracture surface data. We acknowledge useful discussions with D. Bonamy. E.B. is supported by the Horowitz Complexity Science Foundation. This work was supported in part by the Israel Science Foundation administered by the Israel Academy of Sciences.

---

- [1] For a review see: L. Biferale and I. Procaccia, Phys. Rep. **414**, 43 (2005).
- [2] B. B. Mandelbrot, D. E. Passoja and A. J. Paullay, Nature (London) **308**, 721 (1984).
- [3] Cf. E. Bouchaud, Surface Rev. and Lett. **10**, 797 (2003) and references therein.
- [4] J.-J. Ammann and E. Bouchaud, Eur. Phys. J. AP **4**, 133 (1998).
- [5] A. Sagiv, Ph.D. thesis, The Hebrew University of Jerusalem (2005).
- [6] E. Bouchbinder and I. Procaccia, “Fracture Surfaces as Multiscaling Graphs”, submitted to Phys. Rev. Lett. , see also: cond-mat/0508183 (2005).
- [7] I. Arad, V. S. L’vov and I. Procaccia. Phys. Rev. E **59**, 6753 (1999).